Forest Canopy Cover and Height From MISR in Topographically Complex Southwestern US Landscapes Assessed With High Quality Reference Data

Mark Chopping, Malcolm North, Jiquan Chen, Crystal B. Schaaf, *Member, IEEE*, J. Bryan Blair, John V. Martonchik, and Michael A. Bull

***Abstract*—This study addresses the retrieval of spatially contiguous canopy cover and height estimates in southwestern US forests via inversion of a geometric-optical (GO) model against surface bidirectional reflectance factor (BRF) estimates from the Multi-angle Imaging SpectroRadiometer (MISR). Model inversion can provide such maps if good estimates of the background bidirectional reflectance distribution function (BRDF) are available. The study area is in the Sierra National Forest in the Sierra Nevada of California. Tree number density, mean crown radius, and fractional cover reference estimates were obtained via analysis of QuickBird 0.6 m spatial resolution panchromatic imagery using the CANopy Analysis with Panchromatic Imagery (CANAPI) algorithm, while RH50, RH75 and RH100 (50%, 75%, and 100% energy return) height data were obtained from the NASA Laser Vegetation Imaging Sensor (LVIS), a full waveform light detection and ranging (lidar) instrument. These canopy parameters were used to drive a modified version of the simple GO model (SGM), accurately reproducing patterns of MISR 672 nm band surface reflectance (mean RMSE $= 0.011$, mean $\mathrm{R}^2 = 0.82$, $\mathrm{N} = 1048$). Cover and height maps were obtained through model inversion against MISR 672 nm reflectance estimates on a 250 m grid. The free parameters were tree number density and mean crown radius. RMSE values with respect to reference data for the cover and height retrievals were 0.05 and 6.65 m, respectively, with R^2 of 0.54 and 0.49. MISR can thus provide maps of forest cover and height in areas of topographic variation although refinements are required to improve retrieval precision.**

Manuscript received September 23, 2011; revised November 21, 2011; accepted December 15, 2011. Date of publication February 16, 2012; date of current version February 29, 2012. This work was supported by National Aeronautics and Space Administration Grant NNX08AE71G and Grant NNX11AF90G.

M. Chopping is with the Department of Earth and Environmental Studies, Montclair State University, Montclair, NJ 07043 USA (corresponding author, e-mail: chopping@pegasus.montclair.edu).

M. North is with the USDA Forest Service, Pacific Southwest Research Station, Davis, CA 95618 USA (e-mail: mnorth@ucdavis.edu).

J. Chen is with the Department of Environmental Sciences, University of Toledo, Toledo, OH 43560 USA (e-mail: jiquan.chen@utoledo.edu).

C. B. Schaaf is with the Department of Environmental, Earth, and Ocean Sciences, University of Massachusetts, Boston, MA 02125 USA (e-mail: crystal.schaaf@umb.edu).

J. B. Blair is with the NASA Goddard Space Flight Center, Laser Remote Sensing Laboratory, Greenbelt, MD 20771 USA (e-mail: james.b.blair@nasa.gov).

J. V. Martonchik and M. A. Bull are with the NASA Jet Propulsion Laboratory, Pasadena, CA 91109 USA (e-mail: john.v.martonchik@jpl.nasa.gov; michael.a.bull@jpl.nasa.gov).

Color versions of one or more of the figures in this paper are available online at http://ieeexplore.ieee.org.

Digital Object Identifier 10.1109/JSTARS.2012.2184270

***Index Terms*—Biomass, canopy, forestry, lidar, modeling, multi-angle, topography.**

I. Introduction

THIS study uses high quality reference data derived from high spatial resolution (0.6 m) panchromatic imagery and full waveform lidar to investigate the accuracy with which forest canopy cover and height can be retrieved by adjustment of a geometric-optical canopy reflectance model against multiangle 672 nm reflectance data from MISR, a moderate resolution imager on NASA's Terra satellite. Forest canopy cover and height are important first-order canopy structure parameters in basic and applied ecological research. They reflect tree density, successional stage, canopy response to stand-replacing fires and other disturbance, forest health, susceptibility to fire, species distribution, wildlife habitat, and carbon storage in aboveground woody biomass. In the southwestern United States the need for forest canopy cover, height, and biomass mapping capabilities has never been more pressing, with open canopy forests expected to come under increasing stress from climate-related disturbance, e.g., unusually severe and extensive wildfires, mortality from insect and pathogen outbreaks, as well human population and management factors (e.g., grazing, fire suppression) in the coming decades [1]–[6]. Since the mid-1970s the southwestern US has warmed rapidly and precipitation has decreased leading to more intense drought [7]; moreover, there is a consensus that trends towards warming and increased potential evapotranspiration will cause negative water balances by the middle of the century [8], [9]. This will affect forests importantly: higher elevations—where most southwestern forests exist—have experienced greater warming than low elevations. The implication is that if temperature and aridity follow their expected trajectories, these forests will experience substantially reduced growth during this century [6]. Warmer winters and earlier melting of the snowpack and drying of soils and fuels in the spring are already linked to increasingly extensive and severe wildfires in western U.S. forests [1]. Some fires are stand-replacing whereas others are less damaging: canopy cover and height maps can help in remotely determining the severity of a burn. In addition, cover and height are important for assessing habitat. For example, current management on all Sierra Nevada National Forests

uses canopy cover and tree size guidelines based on the need to provide habitat for sensitive species such as the California spotted owl (*Strix occidentalis occidentalis*). At present the Forest Service often estimates habitat suitability from sparse plot data using a model, the Forest Vegetation Simulator [10].

Lidar, radar, and passive multiangle imaging all have a role to play in mapping these forest parameters at regional scales. For example, the Geoscience Laser Altimeter System—a large footprint profiling waveform lidar that was flown on the Ice, Cloud, and land Elevation Satellite—has provided good estimates of canopy height over large areas [11] but did not provide contiguous mapping. Airborne instruments such as the NASA Laser Vegetation Imaging Sensor (LVIS, [12]) can provide robust, precise, and contiguous estimates of canopy height and other structural measures [13] but only sporadically and over relatively small areas. Radar data can provide estimates of canopy height when additional elevation data are available [14]; and aboveground biomass when calibrated with lidar or ground measurements [15]. Multiangle passive solar wavelength reflectance data from moderate resolution instruments provides a third option that has some advantages but also presents important challenges, discussed below.

For assessing changes in forest at regional scales and larger it is necessary to adopt an approach that will provide information on a regular basis and with as long a record as possible. The estimates must have both the accuracy and precision sufficient to differentiate real from spurious trends and to resolve changes from forest degradation or re-growth as well as large changes from harvesting or fire. It is relatively straightforward to detect total forest loss from a large, severe wildfire with a technology that provides a cover estimation precision of $\pm 30\%$ but it would be impossible to say anything meaningful about gradual or subtle changes, such as those arising from selective logging and recovery, especially over periods of less than 10 years. This implies that there is utility in data from moderate resolution instruments (i.e., those with instantaneous fields-of-view (IFOVs) of 100–300 m) that provide a long record and have good spatial and temporal coverage. However the data are difficult to interpret in terms of structural attributes such as canopy cover and height; canopy physical quantities must be inferred from variation in the remotely-sensed signal with respect to wavelength, polarization, and/or viewing and illumination angles, rather than from information available in the spatial domain, as with photogrammetric methods. Moreover, the results are difficult to validate because of the large ground resolution element of $>=$250 m: it is difficult and expensive to obtain ground-based measurements that cover the range of conditions sufficiently well. Plot data that may be used with high- and medium-resolution imagery—such as the U.S. Forest Service's Forest Inventory Analysis (FIA) survey data—are at the wrong scale for use with moderate resolution imagery because the 36 m diameter FIA plot size is almost an order of magnitude too small.

There are several approaches to mapping canopy cover and height over large areas using moderate resolution multiangle satellite remote sensing but they may be divided into two broad categories: empirical and physical. The empirical approach relies on calibration of models whose parameters while potentially meaningful are not physical quantities (e.g., the coefficients of a regression equation or the connection weights used in an artificial neural network). The physical approach exploits models that describe the variation in the remotely-sensed signal with respect to wavelength, polarization, and/or viewing and illumination angles. Both categories involve models of varying complexity, from simple to highly complex and with few or many parameters. Heiskanen [16] and Kimes *et al.* [17] provide examples of empirical approaches to interpretation of multiangle data (exploiting regression and artificial neural networks, respectively); while Widlowski *et al.* [18], Schull *et al.* [19], Zeng & Schaepman [20], Chopping *et al.* [21]–[23], Wang *et al.* [24], and Laurent *et al.* [25] are some examples of physical approaches (BRDF models, geometric-optical models, directional escape probabilities). These studies have shown that it is possible to access the information on canopy structure that is encapsulated in multiangle reflectance data.

The approach pursued in this study involves adjusting a geometric-optical (GO) model in a framework in which the contribution of the (non-tree) background at different viewing and illumination angles is estimated for each location using a dynamically-estimated bidirectional reflectance distribution function (BRDF), rather than a static surface BRDF or brightness value [21]–[23]. A BRDF model provides both reflectance magnitude and anisotropy (i.e., the angular distribution of the outgoing radiation field with respect to the surface and the solar direction), rather than only the isotropic, or diffuse, scattering component. Specification of the background BRDF—or at least the part of it corresponding to the viewing and illumination angles of the observations—is critical for accurate GO canopy reflectance modeling. The background has long been recognized as an important component of the remote sensing problem [26], [27] and remains an area of active research [28]. In this study the background BRDF is estimated via least-squares regression, using the kernel weights of a BRDF model that has been adjusted against the available set of bidirectional reflectance factor (BRF) observations.

Two previous published studies have demonstrated the utility of red band multiangle BRF data from MISR in such a GO model inversion framework (hereafter termed MISR/GO) for forest canopy mapping. In a first study over an area of $\sim$200,000 km^2 in New Mexico and Arizona, retrievals of fractional cover (*fcov*) and mean canopy height were assessed against United States Department of Agriculture, Forest Service Interior West (FS-IW) map series [21]. However the FS-IW estimates were derived using an empirical modeling technique that ingested moderate resolution multispectral products from the NASA MODerate resolution Imaging Spectroradiometer (MODIS), as well as other geospatial inputs and so are not suitable for validation purposes, especially for structural parameters such as canopy height [22], [29]. A second study assessed canopy height retrievals against high resolution discrete return lidar heights from the NASA Cold Land Processes Experiment (CLPX) in the Colorado Rockies. Forest height RMSE distributions with respect to the CLPX lidar estimates were centered between 2.5 and 3.7 m while R_2 distributions were centered between 0.4 and 0.7 $(N = 57)$ [22].

While good compatibility was found between MISR/GO cover, height, and aboveground biomass retrievals and the FS-IW estimates and height retrievals were accurate with respect to high resolution lidar height measurements, initial

TABLE I
DATA SETS USED

Date [1]	Extent (ha)	Description	Filename(s)
-	652,406 [2]	MISR Ancillary Geographic Product	MISR_AM1_AGP_P041_F01_24.b60-61.hdf
08/11/08	652,406 [2]	MISR 1.1 km LAND Product	MISR_AM1_AS_LAND_P041_O046009_F07_0022.b60-61.hdf
08/11/08	652,406 [2]	MISR Geometric Parameters Product	MISR_AM1_GP_GMP_P041_O046009_F03_0013.b60-61.hdf
08/11/08	652,406 [2,3]	MISR Terrain-projected Spectral Radiance	MISR_AM1_GRP_TERRAIN_GM_P041_O046009_nn_F03_0024.b60-61.hdf
09/26/08	6,536 [4]	LVIS Canopy and Ground Elevation	LVIS_US_CA_day4_2008_VECT_20081120.lge
06/25/03	7,380 [5]	QuickBird 0.6m Panchromatic Image	03JUN25183856-P2AS_R2C1-052222275010_01_P001.TIF

[1] Date of acquisition by the remote sensing instrument.
[2] MISR blocks 60 – 61 were mapped into the area bounded by 37° 10' 34"N, 119° 17' 40"W by 36° 31' 26"N, 118° 18' 22"W.
[3] nn indicates the codes for the nine MISR cameras (AN, AA, AF, BA, BF, CA, CF, DA, DF).
[4] Irregular area sampled; the validation area corresponded to the area of the QuickBird subset minus the NE and SW corners where no LVIS data were acquired.
[5] The area is bounded by 37° 01' 18"N, 119° 09' 09"W by 36° 57' 00"N, 119° 02' 57"W.

attempts to map the entire southwestern US using a MISR/GO method produced anomalous results in some places. For example, in locations where the topography is complex and sometimes extreme, cover was severely overestimated and height severely underestimated [30]. This can happen because of the non-uniqueness of solutions when adjusting a model using numerical methods and the pattern of modeled BRFs is very similar with different parameter sets (i.e., the same minimum error within the defined convergence precision can be obtained with more than one solution). Such artifacts may be owing to model inadequacy, poor estimates of the background BRDF, geometric effects of topography, residual atmospheric or intrinsic noise in the BRF data, and/or problems with the inversion protocol (e.g., sensitivity to the starting point).

This study uses robust high quality reference data derived from analysis of high spatial resolution (0.6 m) panchromatic imagery and full waveform lidar to investigate the precision and accuracy with which forest cover and height can be retrieved by adjustment of a GO model against multiangle reflectance data from MISR. Lidar data acquired from the air provide the best means of adequately assessing MISR/GO height retrievals; in this study height metrics from the NASA LVIS full waveform lidar with a nominal spot size of 20 m were used. Accurate estimates of tree density and crown cover, as well as first order tree heights from shadowing were provided by the CANopy Analysis with Panchromatic Imagery (CANAPI) algorithm that was developed to provide maps of these parameters using high spatial resolution (0.5–1 m) panchromatic imagery [31]. These data are required for validation of MISR/GO retrievals and also to drive forward-modeling runs that provide an indication of whether the model is able to accurately reproduce BRF patterns at MISR observation geometries; they are described more fully below.

II. METHODS

In this study tree number density, mean crown radius derived from QuickBird imagery with CANAPI and canopy height from analysis of LVIS waveforms were used to drive a geometric-optical canopy reflectance model in forward mode (to test the ability of a model to predict the 672 nm wavelength radiation field above the canopy as seen by MISR)—as well as in inverse mode (to extract background BRDFs for calibration of the regression models that provide the weights required for calculation of the background contribution for each location, prior to adjusting the model to obtain fractional crown cover and mean canopy height). The following sections describe the data and procedures followed. Please see Table I for a list of the data sets used and their spatio-temporal extents.

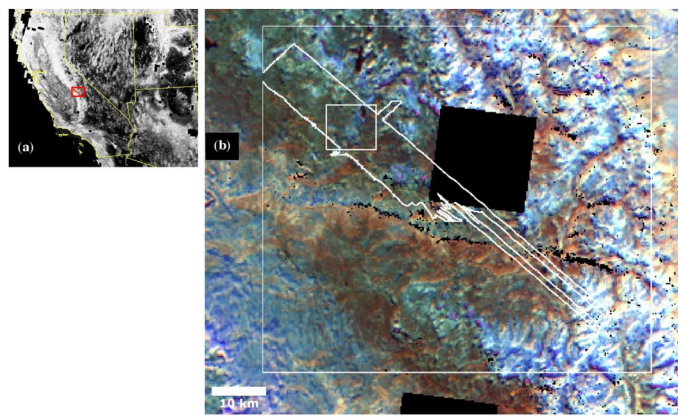

Fig. 1. The location of the study area in the Sierra Nevada National Forest in California, USA (a) over a crown cover map (b) MISR multi-angle composite (RGB = *vol, geo, iso* kernel weights). The irregular area indicates the area surveyed by LVIS on day 4 of the September 2008 campaign. The small rectangle shows the extent of the area used to collect high quality reference data. Black indicates data missing owing to cloud.

A. Study Area

The study area is centered on the area surveyed by LVIS in September 2008 in the Sierra National Forest in the southern Sierra Nevada Mountains of California, USA (Fig. 1). It encompasses an area of 65,625 ha (37° 10′ 34″ N, 119° 17′ 40″ W by 36° 31′ 26″ N, 118° 18′ 22″ W) with elevation ranging from ~850 to 2,700 m. The area includes upland forest in the western part and high desert grassland and scrub in the eastern part. The upland area covers a wide range of vegetation associations including fir, pine, mixed conifer, mixed hardwood and conifer forests sparsely interspersed with meadows. Common tree species include red fir (*Abies magnifica*), white fir (*Abies concolor*), ponderosa pine (*Pinus ponderosa*), Jeffrey pine (*Pinus*

jeffreyi), and incense cedar (*Calocedrus decurrens*) [32]. Tree canopy cover can range from completely open in meadows, rocky ridges, and scree slopes to very dense (but rarely exceeding 50%, or fractional cover $= 0.5$). The topography is highly variable, often complex, and sometimes extreme, with many steep slopes, some well over 40°. There is high variation in slope and aspect within 250×250 m mapped MISR cells, with standard deviations between 0°–13° (slope) and 2°–158° (aspect). On the mountain range precipitation ranges from 500–2030 mm during fall, winter, and spring and occurs mostly as snow above 1828 m. Summers are dry with low humidity, and temperature averages 5.5–15.5°C with a growing season lasting 20–230 days. On the foothills precipitation ranges from 510–1020 mm, temperature averages 13–18°C, and the growing season lasts 200 to 320 days [33].

B. MISR Data Sets and Processing

The MISR instrument is flown on Terra, the first of NASA's Earth Observing System satellites that was launched in December 1999. The instrument consists of nine pushbroom cameras arranged to view along-track that acquire image data with nominal view zenith angles relative to the surface reference ellipsoid of 0.0°, ±26.1°, ±45.6°, ±60.0°, and ±70.5° (forward and aft of the Terra satellite) in four spectral bands (446, 558, 672, and 866 nm) at 1.1 km spatial resolution. The 672 nm (red) band images are also acquired with a nominal maximum cross-track ground spatial resolution of 275 m in all nine cameras and all bands are acquired at this resolution in the nadir camera [34]. Except as otherwise noted, MISR data products are obtained using the MISR Order and Customization Tool hosted at the NASA Langley Atmospheric Science Data Center (http://l0dup05.larc.nasa.gov/MISR/cgi-bin/MISR/main.cgi).

The high resolution (275 m) surface BRF is obtained by first performing a linear regression of the red band 1.1 km MISR surface BRFs against the red band 1.1 km MISR top-of-atmosphere BRFs to obtain the regression coefficients for each of the nine camera view data sets. The regression is performed on the data within each 17.6 km region, producing a grid of regression coefficients, which then are smoothed to eliminate discontinuities between regions. The smoothed regression coefficients are then applied to the red band 275 m top-of-atmosphere MISR BRFs to produce red band 275 m land surface BRFs at the nine camera angles. Top-of-atmosphere BRFs contaminated by sun glint from water surfaces are excluded from input to the regression coefficient calculations.

The surface BRF regression algorithm utilizes four MISR data products: the MISR Level-1B2 Terrain-projected Radiance product (MI1B2T); the MISR Level-1B2 Geometric Parameters product (MI1B2GEOP); the MISR Level-2 Land Surface product (MIL2ASLS); and the Ancillary Geographic product (MIANCAGP). The MI1B2T product provides 275 m terrain-projected top-of-atmosphere radiance in all 4 spectral bands for the nadir view; and in the red band for off-nadir views. Sun and view geometries from the MI1B2GEOP product are combined with a land/water mask from the MIANCAGP product to determine view angles and surfaces susceptible to sun glint. The MIL2ASLS product provides surface BRFs at 1.1 km.

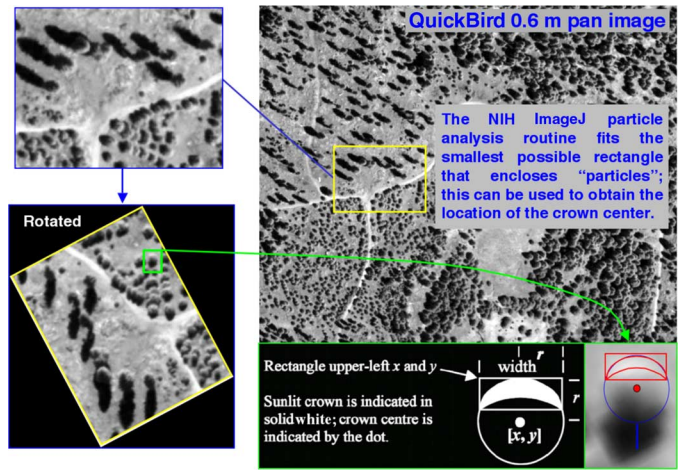

Fig. 2. Schematic showing the principles on which the CANAPI algorithm isolates tree or shrub crowns, finds crown radii, and estimates heights from shadow lengths. The algorithm is implemented in the Image J image processing package from the U.S. National Institutes of Health.

The MISR data used in this study were from Terra orbit 46009 (August 11, 2008), path 41, blocks 60–61. The data were resampled onto a 250 m grid in the Universal Transverse Mercator projection, Zone 11N, WGS84 spheroid/datum. The latest operational MIL2ASLS product (version 22) available from the Langley data center lacked adequate coverage in the study area, primarily due to a topographic complexity constraint imposed by the MISR aerosol algorithm ([35], sections 3.3.1.2.2 and 3.3.8.2.5). Relaxing the regional and subregional topographic complexity thresholds to 1000 m (from 500 m and 250 m, respectively), substantially improved coverage in mountainous regions. Additional coverage was gained by allowing the aerosol retrieval to proceed without the ±70.5° views, when doing so improved coverage. This latter modification is also relevant in mountainous regions due to topographic obscuration of the oblique camera views. The improved MIL2ASLS product was used as input to the surface BRF regression.

C. Forest Canopy Cover and Statistics From Panchromatic Imagery

The CANopy Analysis with Panchromatic Imagery (CANAPI) algorithm allows the calculation of estimates of crown cover, mean crown radius, tree number density, background (non-tree) brightness, and tree height, over large areas [31]. The algorithm identifies crowns in high resolution panchromatic imagery by finding the crescent-shaped areas that correspond to illuminated crowns. It accomplishes this by rotating the original image so that the sun direction is at the top and applying normalization and convolution operations to emphasize sunlit crown pixels (Fig. 2). CANAPI produces maps of idealized (circular) crowns, crown centers, radii, and tree height from shadow-following, wherever possible (Fig. 3). Statistics such as tree number density and mean crown radius can then be calculated for a window of user-selected dimensions, with the mean radius calculated after removing a few values at the edge of the distribution because the maximum is often the result of misidentification of several crowns as one and the minimum is constrained by pixel size.

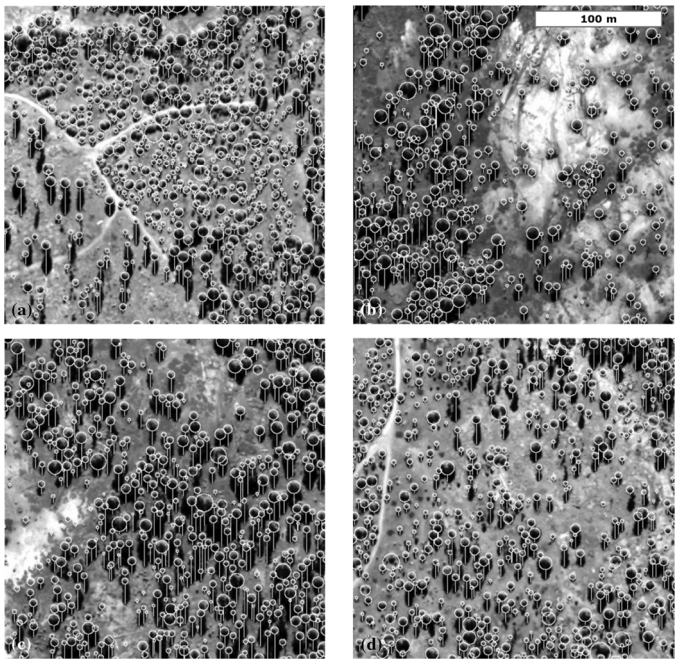

Fig. 3. Typical CANAPI crown (circle) and tree shadow (line) detections over QuickBird 0.6 m panchromatic images in the Teakettle Experimental Forest, Sierra National Forest, California. Shadows that are truncated by tree crowns or the edge of the image are not used in tree height calculation. The imagery was acquired June 25, 2003.

Here, CANAPI estimates of number density and mean crown radius were calculated for 250×250 m windows corresponding to mapped MISR cells, using QuickBird 0.6 m spatial resolution panchromatic imagery acquired on June 25, 2003. The area corresponds to 32×34 MISR cells, providing a reference data set with $N = 1088$. This particular image was selected because it is one of the few available that provides extensive views of the surface during the summer season. There is the possibility that the forest may have changed over the five-year period between the acquisition of the QuickBird imagery and the other data sets, owing to disturbance. In Sierra Nevada mixed conifer forest the main disturbances affecting canopy conditions are fire and bark beetle mortality; wind damage, pests and snow breakage are very rare, localized events. While it is not absolutely certain that there were no major disturbance events in the validation area over the 2003–2008 period, this seems unlikely: it is known that there were no fires in the Teakettle Experimental Forest, a 1300 ha old growth watershed about 2 km to the east that has been intensively studied (e.g., [36]). Bark beetles and other pests and pathogens were studied at Teakettle over this period [37]: while there were chronic levels of bark beetle damage these affected a very small fraction of trees and there were no significant droughts—which are a catalyst for increased beetle mortality—during this period. In the absence of these major disturbances there were likely only small changes in primary forest canopy structural properties (crown cover, mean height) over the period June 2003–September 2008.

CANAPI provides very accurate estimates of fractional cover. When these estimates were compared with those derived from the extensive and detailed Teakettle Ecosystem Experiment (TEE) database of field measurements collected between 1998 and 2001 for fifteen 200 m^2 plots [36], they yielded an absolute RMSE of 0.03 and an adjusted R^2 of 0.92, significant at the 99% level [31]. Maximum CANAPI-derived heights showed a good spatial agreement with LVIS RH100 (100% energy return) maximum canopy height estimates interpolated onto a 20 m grid, although the CANAPI map includes far fewer very tall trees and the relationship was rather weak over the entire range of RH100 values, with obvious underestimation and anomalies at low and high values owing to the inability to obtain heights for all trees falling in the calculation window (shadows may be truncated by crowns or the edge of the window). However when the range 3 m to 60 m (61% of the total) was considered then the R^2 was 0.94, significant at the 99% level, with a relative RMSE of 0.25 and an absolute RMSE of 13.9 m that reflects the divergence from the 1:1 line [31].

D. Lidar Canopy Heights

The lidar data used in this study were collected by the Laser Vegetation Imaging Sensor (LVIS) [12]. LVIS is a full-waveform laser altimeter system optimized to measure canopy structure across large areas. In September of 2008, as a part of an experiment for NASA's Deformation, Ecosystem Structure and Dynamics of Ice (DESDynI) mission, LVIS mapped a large portion of the Sierra National Forest with a 1–2 km wide swath in a series of parallel flight tracks (Fig. 1). Flying at high altitude LVIS produced millions of (nominally 20-m diameter) footprints at the surface. The data from the LVIS surveys used here were collected on Day 4 of the campaign (September 26, 2008) and cover approximately 7,400 ha (37° 01′ 16″N, 119° 09′ 09″W by 36° 56′ 60″N, 119° 02′ 58″W). They are entirely within the area covered by the MISR imagery. The waveforms were analyzed by the LVIS science team to provide ground elevation and canopy height estimates and made available via the LVIS web server at NASA Goddard Space Flight Center [38]. The products used were the ground elevation estimates ("LGE") with respect to the International Terrestrial Reference Frame 2000 (horizontal coordinates)/WGS84 Ellipsoid (vertical coordinates) and the canopy relative height metrics RH50, RH75, and RH100 ("LCE"). In the LVIS product, the height at which the indicated percentage of energy has been returned is estimated; thus RH100 is a measure of maximum tree height within the lidar footprint while RH50 is the height of median energy (HOME). RH75 is the height at which 75% of the energy is returned to the sensor. The mean incidence angle of the LVIS data set was 2.8° with a standard deviation 1.4°; none of the data were acquired at an incidence angle greater than 10°. The LVIS RH50, RH75, and RH100 values within each mapped MISR 250×250 m cell were averaged to obtain first-order canopy height reference data sets, thus these data are not original LVIS data but quantities derived from them. The LGE elevations were used to construct a 37 m horizontal resolution digital elevation model (DEM, Fig. 4) that was used to effect first-order corrections to the RH100 values for slope.

E. Modified Simple Geometric-Optical Model

Geometric-optical (GO) models are able to resolve statistical distributions of discrete objects within an instrument's instan-

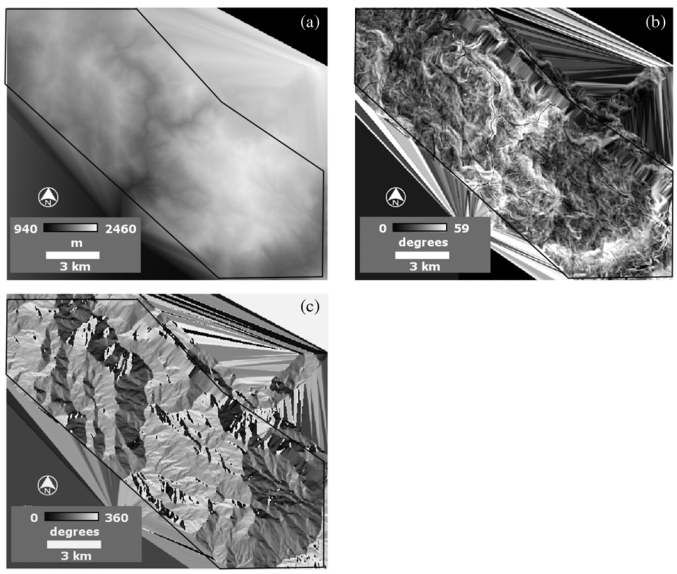

Fig. 4. Topography of the Sierra National Forest study site (a) digital elevation model (DEM) using linear interpolation on LVIS ground returns (b) slope map generated from the DEM (c) aspect map generated from the DEM. Only valid data in the center of the maps—as shown by the solid lines—were used.

taneous field-of-view (IFOV) [39]. Simple geometric-optical models treat the surface as an assemblage of discrete objects of equal radius, shape and height, evenly distributed within a spatial unit. A tree or shrub crown is represented by a spheroid whose center is located at a specified mean height above a background with defined reflectance magnitude and anisotropy (i.e., the background is represented by a BRDF model). These models predict the top-of-canopy reflectance response to important canopy physical parameters (e.g., plant number density, foliage volume, mean canopy crown height, radius, and crown shape, background brightness and anisotropy) as a linear combination of the contributions from sunlit and viewed, and shaded and viewed crown and background components [40], [41]:

$$R = G.k_G + C.k_C + T.k_T + Z.k_Z \tag{1}$$

where R is bidirectional spectral reflectance factor; k_G, k_C, k_T and k_Z are the GO modeled proportions of sunlit background, sunlit crown, shaded crown and shaded background, respectively; and G, C, T, and Z are the contributions of the sunlit background, sunlit crown, shaded crown, and shaded background, respectively. GO functions have been used in Li-Ross BRDF models [42], [43] and are particularly appropriate for the exploitation of solar wavelength remote sensing data acquired at differing viewing and/or illumination angles (i.e., multiangle remote sensing data) because the proportions of sunlit and shaded crown and background in the remote sensing instrument ground-projected IFOV vary with both viewing and illumination angles and canopy configuration.

GO models calculate the proportions of sunlit background (k_G) and crown (k_C) with respect to illumination and viewing directions. These are calculated exactly for the principal and perpendicular planes and approximated away from these, as in (2) and (3), respectively:

$$k_G = \mathrm{e}^{-\lambda\pi \mathrm{r}^2\left\{\sec\vartheta_i' + \sec\vartheta_v' - O(\vartheta_i,\vartheta_v,\varphi)\right\}} \tag{2}$$

$$k_C = \left(1 - \mathrm{e}^{-\lambda\pi \mathrm{r}^2 \sec\vartheta_v'}\right)\frac{1}{2}(1+\cos\varepsilon') \tag{3}$$

where ϑ and φ indicate zenith and azimuth angles where the subscripts i and v indicate illumination and viewing angles; λ is the tree number density; r is the average radius of tree crowns; ε' is the transformed scattering phase angle:

$$\cos\varepsilon' = \cos\vartheta_i' \cos\vartheta_v' + \sin\vartheta_i' \sin\vartheta_v' \cos\varphi \tag{4}$$

and O is the overlap area between the shadows of illumination and viewing [43]:

$$O = 1/\pi(t - \sin t\cos t)\left(\sec\vartheta_i' + \sec\vartheta_v'\right) \tag{5}$$

where t is a parameter that indirectly expresses the locations of the end points of the line that intersects the shadows of viewing and illumination. This allows k_G to be expressed in a way that depends only on the value of t (see [43]). The prime indicates equivalent zenith angles obtained by a vertical scale transformation based on b/r, in order to treat spheroids as spheres [43]:

$$\vartheta' = \tan^{-1}(b/r\tan\vartheta) \tag{6}$$

These functions thus depend on the parameters b/r (vertical crown radius/horizontal crown radius) and h/b (height of crown center/vertical crown radius) which describe the shape and height of the crown. The model's primary structural parameters are therefore: tree number density (λ), mean crown radius (r), crown vertical to horizontal radius ratio (b/r), and crown center height to vertical radius ratio (h/b). The crown signature may be represented by a volume scattering function [44], in which case an in-crown LAI or foliage volume parameter may also be specified.

In this study a modified version of the simple geometric model (SGM), a GO model incorporating a dynamic background (calculated for each location separately), was used [21]–[23]. It is formulated as

$$R = G_{RTLS}(\vartheta i,\vartheta v,\varphi).k_G(\vartheta i,\vartheta v,\varphi) + C_{crown}.k_C(\vartheta i,\vartheta v,\varphi) + S_{TZ}.k_{TZ}(\vartheta i,\vartheta v,\varphi) \tag{7}$$

where ϑ_i, ϑ_v and φ are the view zenith, solar zenith and relative azimuth angles, respectively; k_G, k_C and k_{ZT} are the calculated proportions of sunlit and viewed background and crown, and shaded components (shaded ground and crown), respectively; G_{RTLS} is the background contribution represented by the RossThick-LiSparse-reciprocal (RTLS) BRDF model; C_{crown} is the red wavelength bidirectional reflectance signature for crowns (set at 0.03 in this study); and S_{TZ} is the estimated contribution of shaded components (here set to 0.02). Note that the crown signature differs from the spectral reflectance of fir leaves (∼0.05; [45]) because the observed crown area in the instrument IFOV is not composed simply of leaves but includes non-negligible in-crown shadows. The

crown and shadow signature values are estimated but they are not arbitrary. The model's physical upper canopy parameters are tree number density (λ, trees per square meter), mean crown radius (r), crown vertical to horizontal radius ratio (b/r), crown center height to vertical radius ratio (h/b), and crown spectral reflectance. The model used in this study differs from the previous version in several ways:

- The shaded components T and Z ((1)) that were previously assumed black (as in the kernel-driven BRDF models) are no longer discarded because in these tall forests shaded ground and crown can account for a relatively large proportion of a nadir-viewing instrument's IFOV (Fig. 3(c)); instead they are allocated a signature, S_{TZ}, of 0.02;
- The 3-parameter RTLS BRDF model replaced the 4-parameter modified Walthall model [46], [47] in order to make assessment of extracted and predicted backgrounds more straightforward; and to increase the robustness of background BRDF retrievals (with four kernels it is more likely that their contributions will be confounded);
- The Ross volume scattering function with its in-crown LAI parameter is replaced by a crown red wavelength signature of 0.03, based on a leaf red wavelength reflectance value of 0.05 for fir [45] minus a small decrement to account for in-crown shadows.

F. Isolation of the Background Contribution

The "background" includes everything within the mapped IFOV of the instrument that is not part of the upper canopy and is here typically composed of many elements, possibly including bare soil, rock faces, scree, gravel, crusts, mosses, lichens, and understory plants such as grasses, forbs, and sub-shrubs (Fig. 5). In order to estimate background brightness and anisotropy in the various MISR illumination/viewing configurations, linear multiple regression based on a number of calibration sites was used. The independent variables are RossthiN-LiSparse-reciprocal (RNLS) BRDF model red band isotropic (*iso*), geometric (*geo*), and volume scattering (*vol*) kernel weights, obtained by adjusting the model against MISR red band BRFs in all nine cameras using the Algorithm for Modeling Bidirectional Reflectance Anisotropies of the Land Surface (AMBRALS) code [48], with the objective function $\mathrm{Min}(|\mathrm{RMSE}|)$. Since it is difficult to find 250×250 m areas that are partly vegetated but do not contain shrubs or trees, background contributions must usually be extracted: provided with a set of MISR red band BRFs, estimates of upper canopy statistics from CANAPI (and optionally, LVIS), and the GO model, an optimization algorithm can extract the best-matching background for each site. In other words, when the contribution of the upper canopy in the observed MISR BRF pattern has been accounted for, the remaining contribution must be from the background (Fig. 6). Background BRDFs retrieved in this way are hereafter referred to as "optimal" backgrounds.

Two methods were used to find sets of background RTLS model red band kernel weights (i.e., the dependent variables in the regression equations). First, an automated approach was followed: since CANAPI provides canopy statistics for large areas it is possible to extract kernel weight sets for many contiguous 250×250 m windows corresponding to MISR grid cells.

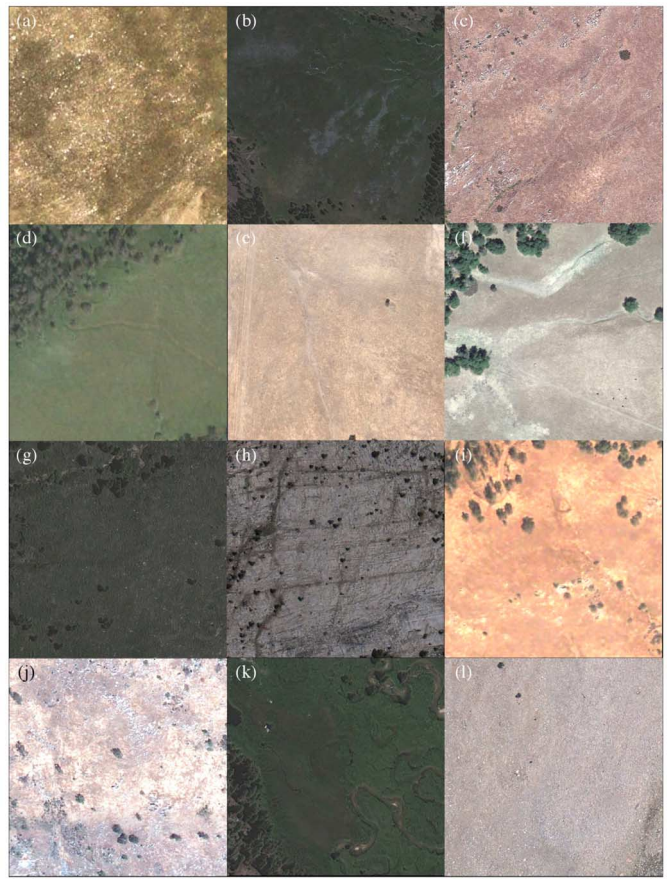

Fig. 5. A selection of 250 x 250 m image chips from Google Earth showing the wide range of non-tree- backgrounds for which the GO modeling framework must attempt to predict BRDF: (a) rocky/stony scrub; (b) meadow with lichens; (c) senescent sparse grasses with rocks; (d) lush meadow; (e) senescent grasses; (f) senescent grasses with exposed soil; (g) low shrubs, rocks/stones, exposed soil, grasses; (h) highly stratified uplifted and tilted rock face; (i) senescent grasses with exposed bright mineral soil; (j) bright exposed caliche with rock outcrops and stones; (k) wet meadow grasses and low shrubs; (l) talus slope.

Here 1048 windows from the part of a QuickBird scene from June 25, 2003 that included LVIS canopy height metrics were used (the "validation area"). To find the optimal backgrounds, for each location the GO model λ and r parameters were set to the CANAPI-derived values, h/b was fixed at 1.0 (typical for conifers), and b/r was adjusted so that mean crown height $(h+b)$ matched the corresponding LVIS RH50 value. RH50 was used because it is more closely related to GO model mean canopy height than RH75 or RH100 [13], [49]. The RTLS background BRDF model kernel weights were then adjusted to minimize the absolute RMSE between the GO model and MISR BRFs. In the second approach, an extensive visual scan of high resolution imagery was performed in Google Earth for the area of the MISR scene, seeking 250×250 m cells with very low (generally $<$10%) canopy cover. The same extraction procedure was followed, though mean crown radius was estimated from the imagery, tree number density set to give a match with fractional cover (measured via thresholding), and b/r was set to 1.0 and 4.0 for broadleaf and coniferous trees, respectively.

Having obtained the best-fitting RTLS background model kernel weights with respect to the MISR data, regression

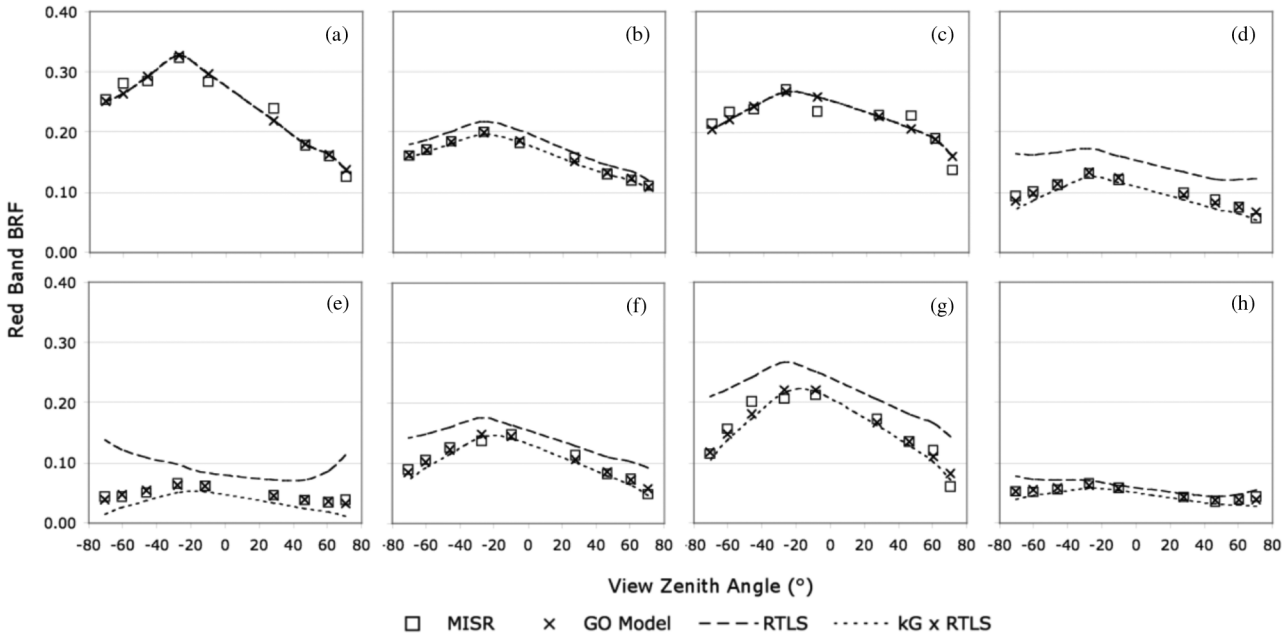

Fig. 6. Observed and modeled MISR red band (672 nm) bidirectional reflectance factor patterns, indicating the contributions from the upper canopy (trees) and the background ($k_G \times \mathrm{RTLS}$, where RTLS indicates the RossThin-LiSparse BRDF model). The background BRDF model kernel weights were adjusted to provide the lowest absolute RMSE between the GO model and the MISR observations. (a) Bare rock; (b) abundant shrubs; (c) sparsely vegetated; (d) broadleaf trees over grass; (e) conifers over grass; (f) ∼10% tree crown cover over rocky surface; (g) ∼5% tree crown cover over rocky surface; (h) ∼5% tree crown cover over lush grass.

coefficients were obtained for each of the model parameters using the RNLS kernel weights as the independent variables. The resulting regression equations can be used to obtain estimates of the background response prior to adjustment of the GO model [21]–[23]. For the automated approach, the set of locations used to obtain the regression coefficients was reduced by considering only those locations where the CANAPI crown cover estimate was $<15\%$.

G. Model Evaluation in Forward Mode

In forward mode the GO model was driven to predict red band BRFs for all available MISR cameras (in these data ranging from six to nine looks but usually eight or nine) for all locations with reference data, using tree number density and mean crown radius from CANAPI; mean b/r from adjustment against LVIS RH100 (because modeled height depends on b/r); and the RTLS BRDF model background (predicted by red band RNLS BRDF model kernel weights). This was accomplished for 1048 of the 1088 250×250 m areas within the QuickBird sub-scene as complete LVIS data were not available for 40 MISR pixels. The resulting BRFs were then compared with the observed patterns from MISR.

H. Model Inversion Protocol

Retrieval of fractional cover and mean canopy height for each mapped grid location was performed by adjusting the model against the MISR data using a numerical optimization algorithm. Forward differencing was used for estimates of partial derivatives of the objective function and a Newton search method was used at each iteration to decide which direction to pursue in the parameter space [50]. The objective function

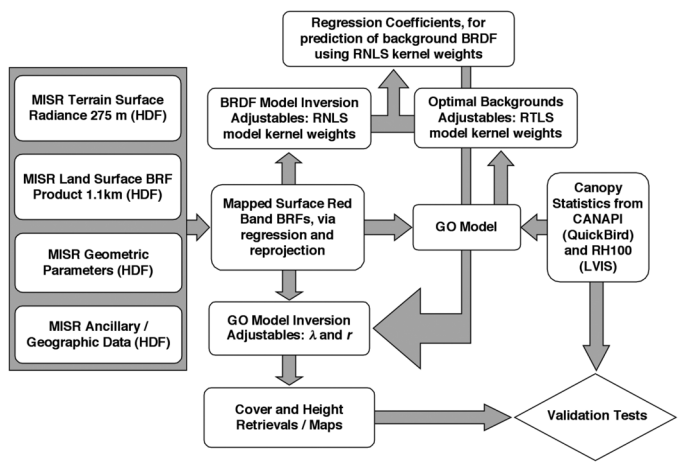

Fig. 7. Flowchart of the operations performed to retrieve and validate fractional crown cover and mean canopy height via GO model inversion against MISR 672 nm band BRFs.

was $\mathrm{Min}(|\mathrm{RMSE}|)$ with no weighting of the error terms with respect to viewing angle. No constraints were imposed. Tree number density (λ) and mean radius (r) were left as adjustable parameters, with h/b and b/r set to 1.0 (typical for conifers) and 4.0 (tall trees), respectively. Retrievals were thus effectively for fractional crown cover (a function of λ and r) and mean canopy height (a function of r, since model height is controlled by the terms h/b and b/r that are both fixed). MISR red band data in all available cameras were used. The number available is usually nine but is occasionally six, seven, or eight.

The initial values of λ and r were set to 0.004 (250 trees per MISR grid cell of 62,500 m^2) and 3.0 m, respectively. Note that

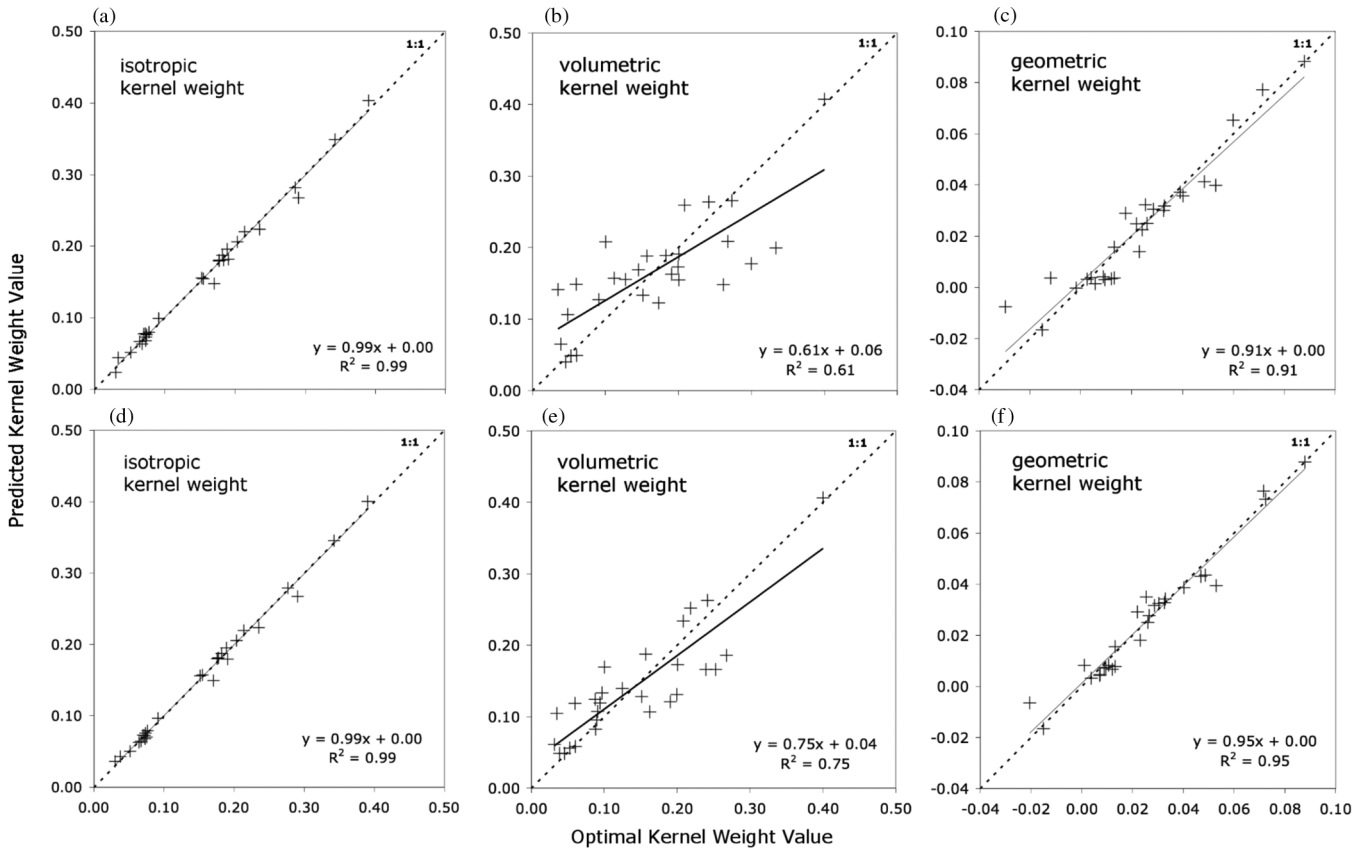

Fig. 8. (a)–(c) Predicted versus optimal background BRDF model red band isotropic, volume, and geometric scattering kernel weights for the 28 background calibration sites; (d)–(f) for backgrounds predicted using kernel weights plus the green and near-infrared BRFs from the MISR nadir camera.

effective values are retrieved: the parameters are internally coupled and the same BRF pattern is obtained if these two parameters are varied with fractional cover maintained, so it is not feasible to adjust both parameters simultaneously to obtain real values. However r also determines mean top-of-canopy height $(h+b)$: since b/r and h/b are fixed, and λ and r are adjusted, the inversion effectively provides an estimate of b (vertical crown radius) allowing the calculation of an estimate of h, via $h/b \times b$, noting that h refers to the mean height of crown centers. Fractional crown cover $(fcov)$ was calculated assuming overlap between crowns, according to the Beer-Lambert law (e.g., [10]):

$$fcov = 1.0 - \exp(-\lambda \times \pi r^2) \tag{8}$$

The retrieved values of λ and r were read into raster image layers for mapping and analysis, along with the model-fitting RMSE, R^2, fractional cover, and top-of-canopy height.

The procedures by which the data and GO model are used to extract background BRDFs and to invert the GO model and validate retrievals are depicted in a flow-chart (Fig. 7).

III. Results and Discussion

CANAPI crown cover within the validation area ranges from 0.0–0.4 and it is therefore clearly critical that the background contribution at the instrument illumination and observation angles is predicted as accurately as possible. This is a challenging task using simple regression methods in view of the diversity of background types and each candidate set of coefficients must be assessed in both forward and inverse modes. Attempts to obtain a regression model using the automated approach in which all 1048 MISR grid cells for which CANAPI λ and r and LVIS RH50 data were available did not produce reasonable inversion results, even when the CANAPI-derived canopy cover was used to restrict the set of locations considered to $<15\%$. There was only a small improvement when combining a low cover set obtained in this way with data from a few individually-selected low cover locations outside the validation area. This may be because the 1048 cells do not cover a sufficiently wide range of background conditions.

Using 28 grid cells selected for low woody plant cover drawn from a larger area provided a much wider variety of background types, as indicated in Fig. 5. The predicted background BRDF model kernel weights rendered R^2 of 0.99, 0.61, and 0.91 for the isotropic, volume-scattering, and geometric kernel weights, respectively, with respect to the optimal weights (Fig. 8(a)–(c)). This is surprisingly good in view of the wide diversity of components that may include stony scrub, lush meadow, exposed soil, low shrubs, exposed soil, uplifted rock faces, rocks of various sizes, caliche, and talus slopes. Only slightly improved results were obtained using kernel weights plus green and near-infrared band BRFs from the MISR nadir camera (Fig. 8(d)–(f)). The regression results show that not all independent variables contributed to accurate results, for example, the RNLS geometric scattering kernel weight was not significant

TABLE II
BACKGROUND KERNEL WEIGHT COEFFICIENTS

	Kernel Weight Regression Coefficients (bold = not significant @ *p*=0.05)		
	Background model (RTLS-Reciprocal)		
Observed (RNLS-Reciprocal)	Isotropic	Volume	Geometric
Intercept	**0.008**	0.133	-0.013
Isotropic kernel weight	0.955	-0.960	0.112
Volume scattering kernel weight	-1.096	**2.879**	-0.489
Geometric kernel weight	**0.334**	3.485	0.641

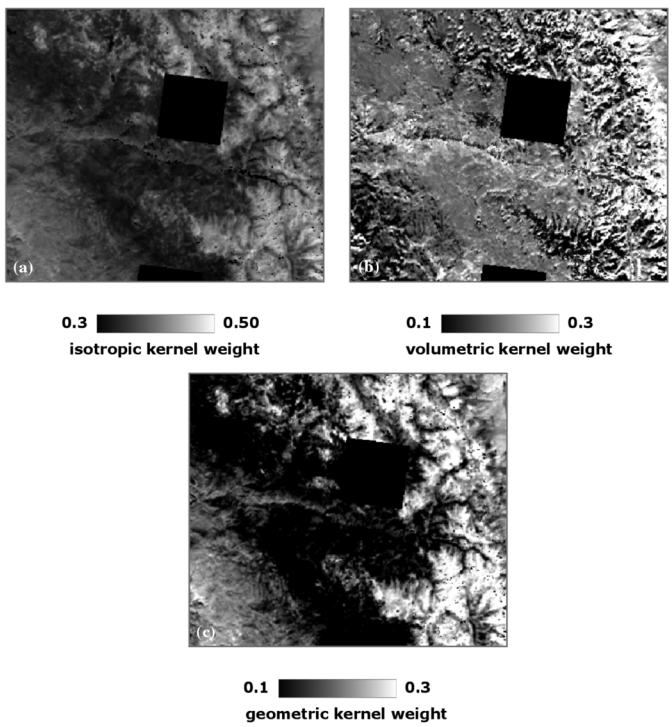

Fig. 9. Maps of the predicted background BRDF model kernel weights: (a) isotropic (diffuse) scattering; (b) volume scattering; (c) geometric scattering.

in predicting the RTLS background model isotropic kernel weight (Table II). Maps of the predicted RTLS background BRDF model kernel weights show reasonable distributions, with higher isotropic kernel weight values for the snow-covered mountain tops in the east-central part of the scene and lower values in densely-vegetated areas (Fig. 9). The geometric kernel weight also shows a strong spatial correspondence with snow cover and is higher over sparse vegetation and lower over densely-vegetated areas, while the volume scattering kernel weight is relatively high over dense vegetation, as expected, although its behavior varies over snow-covered areas.

Comparison of the model-predicted patterns with those from MISR for 1048 locations provided distributions in which 96.6% have $\mathrm{R}^2 > 0.7$ and 97.0% have $\mathrm{RMSE} < 0.02$ [Fig. 10(a), (b)]. When the RMSE and R^2 values are plotted against fractional crown cover it can be seen that there is only a small change in accuracy with cover [Fig. 10(c), (d)], with a mean RMSE of 0.011 and a mean R^2 of 0.82. These results suggest that the GO model is able to predict the sequence of BRFs observed by MISR in all nine cameras rather well, implying that the background prediction is effective. Note however that even if the background prediction were perfect this is no guarantee of accuracy on model inversion: there is still a potentially strong dependence on the optimization algorithm, its scaling and precision settings, and the starting point. The distributions of tree number density (effective), mean crown radius (m; effective), fractional cover (unitless) and mean canopy height (m) are all approximately normal (Fig. 11).

Model adjustment against the MISR red band BRFS resulted in mean (standard deviation) model-fitting RMSE and coefficient of determination values of 0.009 (0.009) and 0.78 (0.199) respectively, with mode values of 0.008 and 0.925 (Table III). The inversion algorithm was thus able to fit the model to the data well. The MISR/GO fractional cover retrievals showed a moderately strong relationship to the CANAPI estimates, with an R^2 of 0.56 [Fig. 12(a)], significant at the 99% level. The RMSE with respect to the CANAPI data is 0.05 over a range that spans 0.01–0.39. The MISR/GO mean canopy height retrievals show a somewhat less strong relationship to the LVIS RH100, RH75, and RH50 data, with R^2 of 0.49, 0.38, and 0.44, respectively [Fig. 12(b)–(d)], all significant at the 99% level. The RMSE with respect to LVIS RH100 is 6.65 meters, considerably higher than that obtained under the less strenuous topographic conditions and lower canopies of the Rocky Mountains in Colorado [22], although in this Sierra Nevada landscape the mean and range are also much larger: 30.1 m, spanning 3.4–62.0 m. There is marked overestimation at low values and underestimation at high values with respect to RH100, noting that the RH100 value indicates the mean of the set of RH100 values within the mapped MISR cells. This bias is less marked in the relationship with RH75 and is almost negligible in the relationship with RH50 [Fig. 12(c) and (d), respectively], which may indicate that it is not reasonable to compare MISR/GO mean canopy heights with the mean of many lidar maximum canopy heights (RH100), even though RH100 provided the best match.

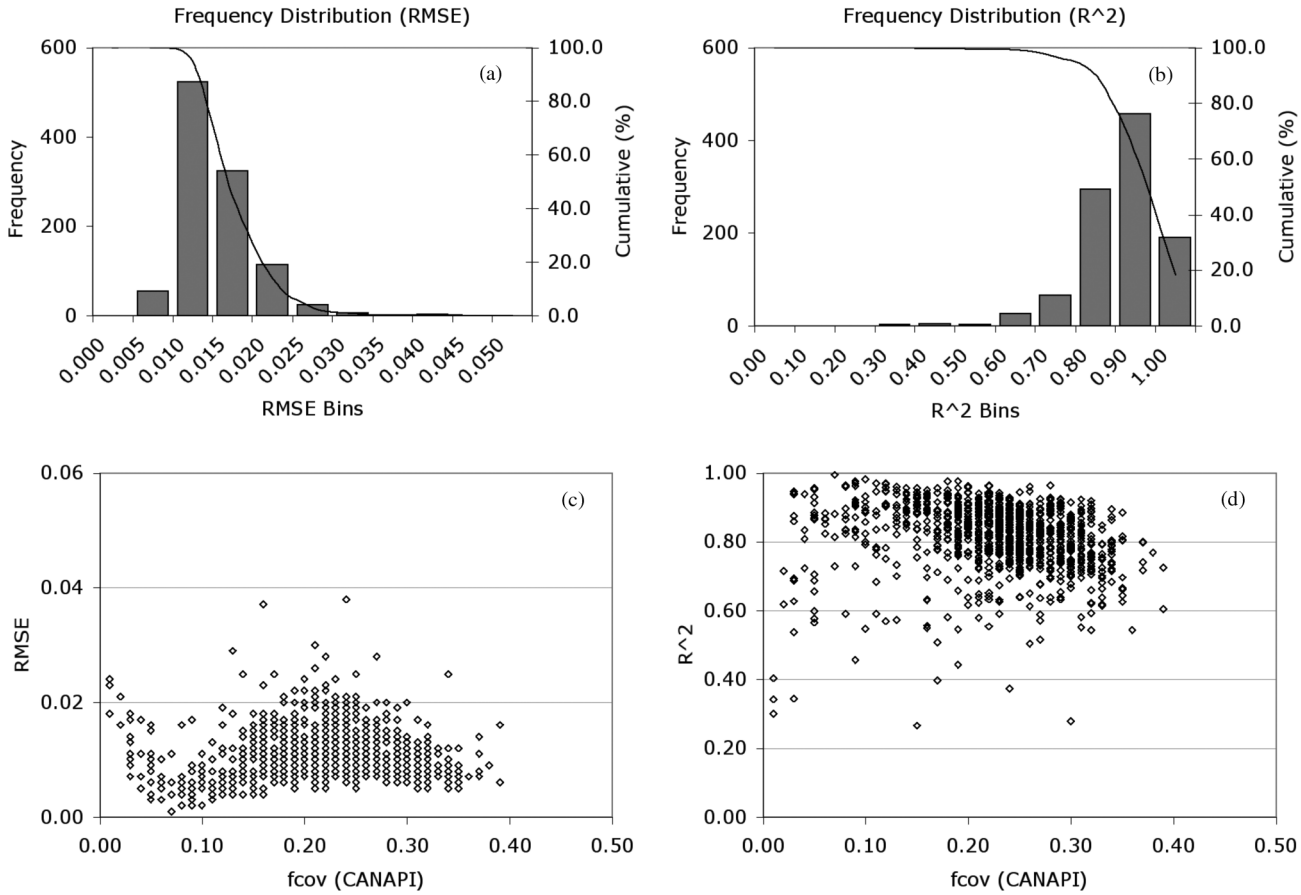

Fig. 10. Results of the GO model predictions when driven by CANAPI tree number density and mean crown radius, LVIS RH100, and the RTLS BRDF model representing the background, for 1048 contiguous locations: (a) histogram of modeled versus MISR RMSE values; (b) histogram of modeled versus MISR coefficient of determination (R^2) values; (c) distribution of RMSE values with respect to CANAPI/QuickBird fractional cover estimates (*fcov*); (d) distribution of R^2 values with respect to CANAPI/QuickBird fractional cover estimates.

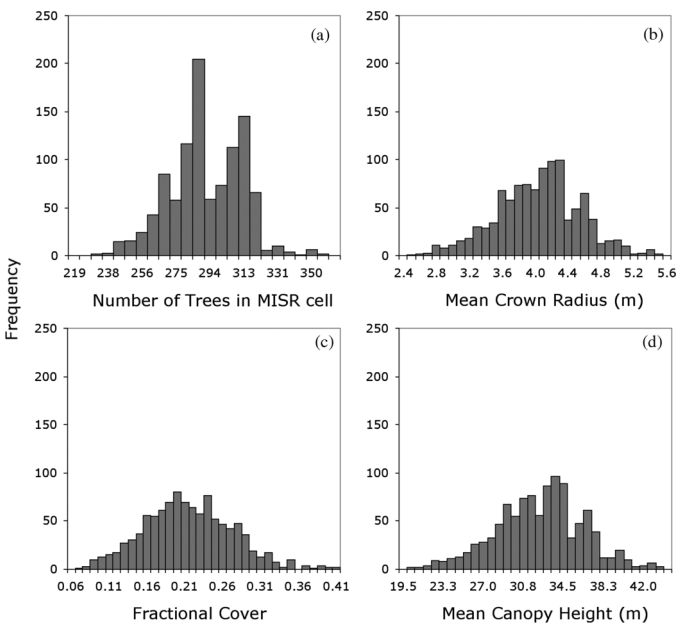

Fig. 11. Histograms for tree number, mean crown radius, fractional cover, and mean canopy height obtained by inversion of the GO model against MISR red band BRFs in all nine cameras.

Representations of typical 250 m grid interval MISR/GO maps of model-fitting RMSE, fractional cover, and mean canopy height are given in Fig. 13, together with a standard false color composite (RGB = Near-Infrared/Red/Green). The missing data in these maps correspond to 17.6 km^2 blocks where the MISR aerosol/surface retrievals failed because of cloud cover. High model-fitting RMSE has been found to indicate contamination by clouds [21], [22] but there is no indication of cloud contamination in this scene, except perhaps in the north-central part; it is also possible that RMSE cannot be used to detect cloud over snow, which also results in high values. The distributions of cover and height values appear reasonable on comparison with features in high resolution imagery in the Google Earth archive, i.e., high (low) canopies appear to have taller (shorter) trees, although this assessment is necessarily qualitative.

TABLE III
SGM INVERSION STATISTICS

	Model-Fitting RMSE	Model-Fitting R^2
Minimum	0.001	0.000
Maximum	0.283	0.999
Mean	0.009	0.775
Mode	0.008	0.925
Standard Deviation	0.009	0.199

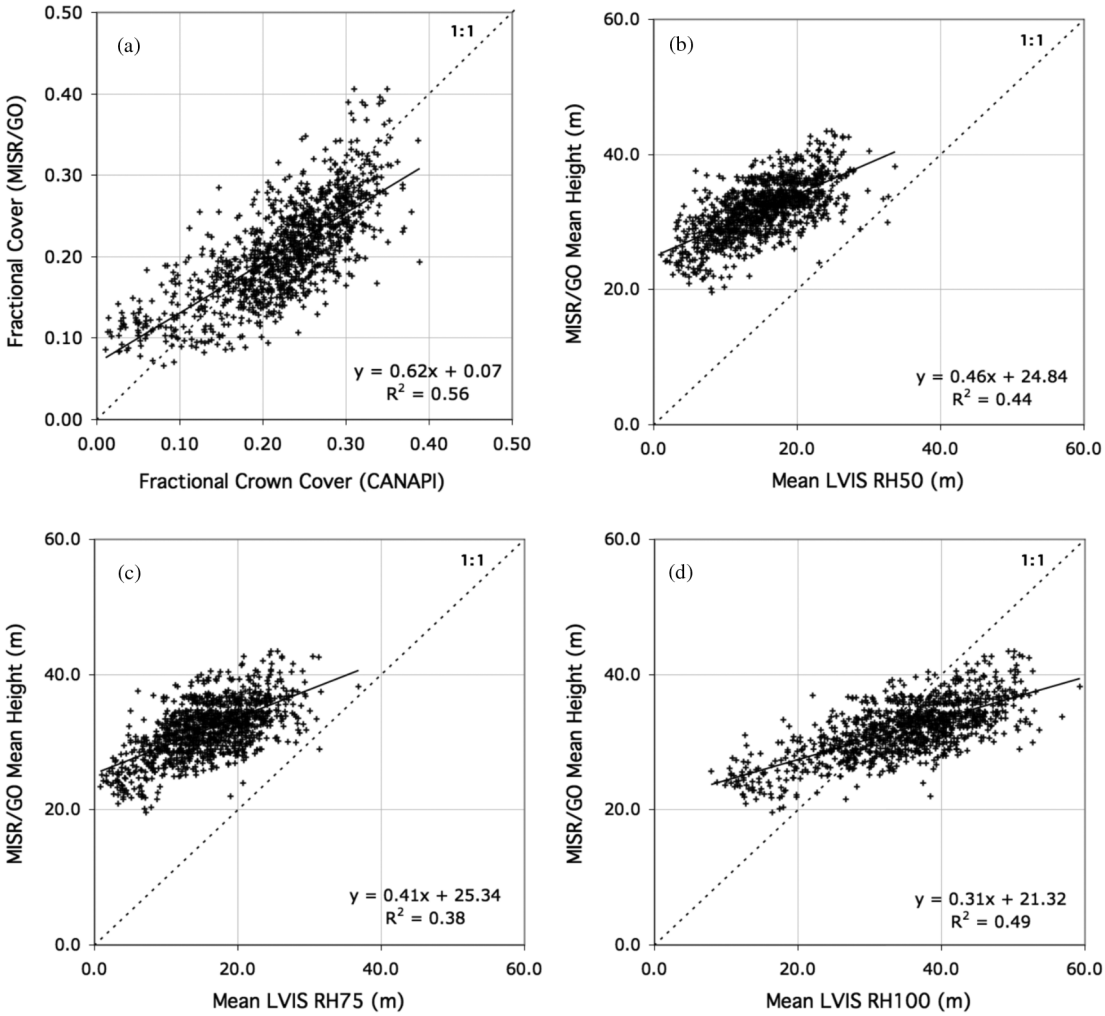

Fig. 12. (a) MISR fractional crown cover from inversion of the GO model versus CANAPI/QuickBird-derived fractional crown cover (b) MISR mean canopy heights with no rescaling versus mean LVIS RH50 canopy heights (average over the 250 × 250 m MISR cell) (c) versus RH75 (d) versus RH100. See Table II for inversion statistics.

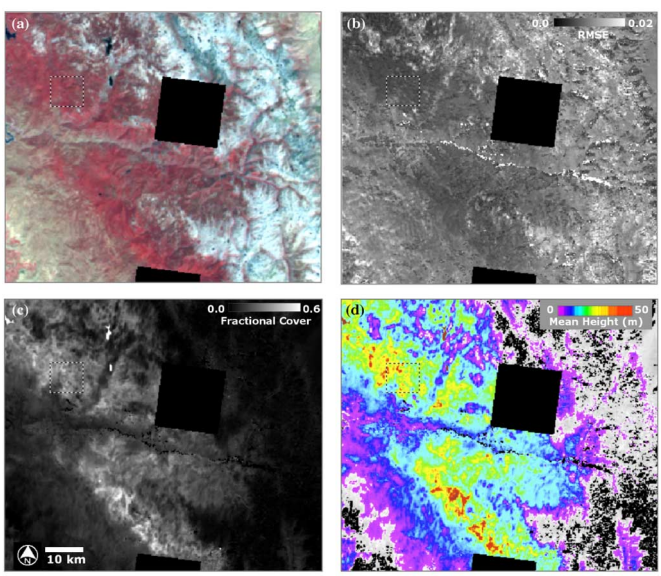

Fig. 13. (a) MISR An (nadir) camera 250 m false color composite with RGB = NIR, Red, Green BRFs (b) 250 m map of RMSE on GO model fitting (c) 250 m map of retrieved fractional crown cover, assuming crown overlap (d) 250 m map of retrieved mean canopy height. The dotted line indicates the validation area for which CANAPI and LVIS data were both available. Black rectangular areas indicate missing data owing to cloud.

IV. Conclusions

This study has demonstrated that multiangle red band surface BRF estimates from MISR can be used to invert a simple geometric-optical canopy reflectance model for mapping canopy cover and height in open forest canopies, even in areas of complex and often severe topography and with a very wide range of background conditions. The retrieved cover and height estimates were obtained independently from the reference data, not via training or empirical relationships. While a part of the signal observed by MISR originates from the background and is obtained via regression, its contribution at any given geometry is based on kernel weights that have a physical meaning. The ability of the modified simple GO model to reproduce observed 672 nm BRF patterns was demonstrated. The use of a non-zero shadow component and a leaf+shadow crown signature instead of the non-linear Ross scattering function provided a realistic model, as shown by the forward-modeling results: when driven with first order canopy structural parameters (tree number density, mean crown radius, LVIS RH100 canopy heights), the modified model reproduced MISR BRF patterns quite accurately. For large area mapping there are some important caveats: the major factor in avoiding anomalous cover and height retrievals was the use of a locally-calibrated background

BRDF, implying that more than one set of calibration coefficients might be required in order to enable accurate GO model inversion for very different landscape types. The study has also shown that is it difficult to obtain high precision in canopy height retrievals in these circumstances, with an RMSE of 6.7 m versus LVIS RH100. This allows only a rather coarse binning of canopy height to obtain high accuracy, although it is still a very useful capability, noting that the range of canopy heights is quite large (the minimum, maximum, and mean heights are 3.4, 62.0, and 30.1 m, respectively). Nevertheless, the study showed that it is possible to leverage moderate resolution multiangle data using a GO model to map forest structural parameters at regional scales; assuming data continuity, this could help to provide a more complete picture of changes in the forests of the southwestern United States as they respond to changing disturbance and management regimes over the coming decades.

ACKNOWLEDGMENT

The authors acknowledge the LVIS team for use of the LVIS data. They thank Xiaohong Chopping for informed comment; Sawahiko Shimada (Agricultural University of Tokyo) for assistance with large-scale BRDF model inversions; and Joseph Youn and Michael Stoppay (Computer Operations for Research and Education, College of Science and Mathematics, Montclair State University) for computing support. They also thank the two anonymous reviewers for their insights on the original manuscript. The MISR data were obtained from the NASA Langley Atmospheric Science Data Center. LVIS data sets were provided by the Laser Vegetation Imaging Sensor (LVIS) team in the Laser Remote Sensing Branch at NASA Goddard Space Flight Center, with support from the University of Maryland, College Park.

REFERENCES

[1] A. L. Westerling, H. G. Hidalgo, D. R. Cayan, and T. W. Swetnam, "Warming and earlier spring increases Western U.S. forest wildfire activity," *Science*, vol. 313, no. 5789, pp. 940–943, 2006, doi 10.1126/science.1128834.

[2] C. I. Millar, N. L. Stephenson, and S. L. Stephens, "Climate change and forests of the future: Managing in the face of uncertainty," *Ecol. Appl.*, vol. 17, no. 8, pp. 2145–2151, 2007.

[3] R. Seager, M. Ting, I. Held, Y. Kushnir, J. Lu, G. Vecchi, H.-P. Huang, N. Harnik, A. Leetmaa, N.-C. Lau, C. Li, J. Velez, and N. Naik, "Model projections of an imminent transition to a more arid climate in southwestern North America," *Science*, vol. 316, no. 5828, pp. 1181–1184, 2007.

[4] D. McKenzie, D. L. Peterson, and J. J. Littell, "Global warming and stress complexes in forests of western North America," in *Wildland Fires and Air Pollution*, A. Bytnerowicz, M. J. Arbaugh, A. R. Riebau, and C. Andersen, Eds. The Netherlands: Elsevier, 2009, vol. 8, Developments in Environmental Science, ch. 15, pp. 319–337.

[5] P. J. van Mantgem, N. L. Stephenson, J. C. Byrne, L. D. Daniels, J. F. Franklin, P. Z. Fulé, M. E. Harmon, A. J. Larson, J. M. Smith, A. H. Taylor, and T. T. Veblen, "Widespread increase of tree mortality rates in the western United States," *Science*, vol. 323, pp. 521–524, 2009.

[6] A. P. Williams, C. D. Allen, C. I. Millar, T. W. Swetnam, J. Michaelsen, C. J. Still, and S. W. Leavitt, "Climate change and water in southwestern North America special feature: Forest responses to increasing aridity and warmth in the southwestern United States," *Proc. Nat. Acad. Sci. USA*, vol. 107, no. 50, pp. 21289–21294, 2010.

[7] D. R. Cayan, T. Dasa, D. W. Pierce, T. P. Barnett, M. Tyree, and A. Gershunov, "Future dryness in the southwest US and the hydrology of the early 21st century drought," *Proc. Nat. Acad. Sci. USA*, vol. 107, pp. 21271–21276, 2010.

[8] IPCC, Synthesis Report. Contribution of Working Groups I, II, and III to the Fourth Assessment Report of the Intergovernmental Panel on Climate Change (Cambridge Univ. Press, Cambridge, UK) 2007.

[9] R. Seager and G. A. Vecchi, "Greenhouse warming and the twenty-first century hydroclimate of southwestern North America," *Proc. Nat. Acad. Sci. USA*, vol. 107, pp. 21277–21282, 2010.

[10] N. L. Crookston and A. R. Stage, "Percent Canopy Cover and Stand Structure Statistics From the Forest Vegetation Simulator," U.S. Department of Agriculture, Forest Service, Rocky Mountain Research Station. 11, Ogden, UT, General Technical Report RMRS-GTR-24, 1999.

[11] M. A. Lefsky, D. J. Harding, M. Keller, W. B. Cohen, C. C. Carabajal, F. D. B. Espirito-Santo, M. O. Hunter, and R. de Oliveira, Jr., "Estimates of forest canopy height and aboveground biomass using ICESat," *Geophys. Res. Lett.*, vol. 32, no. L22S02, 2005, doi 10.1029/2005GL023971.

[12] J. B. Blair, D. L. Rabine, and M. A. Hofton, "The Laser Vegetation Imaging Sensor (LVIS): A medium-altitude, digitization-only, airborne laser altimeter for mapping vegetation and topography," *ISPRS Int. Soc. Photogramm.*, vol. 54, pp. 115–122, 1999.

[13] W. Ni-Meister, S. Lee, A. H. Strahler, C. E. Woodcock, C. Schaaf, T. Yao, K. J. Ranson, G. Sun, and J. B. Blair, "Assessing general relationships between aboveground biomass and vegetation structure parameters for improved carbon estimate from lidar remote sensing," *J. Geophys. Res.*, vol. 115, pp. 148–227, 2010.

[14] J. Kellndorfer, W. Walker, E. LaPoint, and K. Kirsch, "Statistical fusion of Lidar, InSAR, and optical remote sensing data for forest stand height characterization: A regional-scale method based on LVIS, SRTM, Landsat ETM+, and ancillary data sets," *J. Geophys. Res.*, vol. 115, no. G00E08, p. 10, 2010, doi 10.1029/2009JG000997.

[15] E. T. A. Mitchard, S. S. Saatchi, I. H. Woodhouse, G. Nangendo, N. S. Ribeiro, M. Williams, C. M. Ryan, S. L. Lewis, T. R. Feldpausch, and P. Meir, "Using satellite radar backscatter to predict above-ground woody biomass: A consistent relationship across four different African landscapes," *Geophys. Res. Lett.*, vol. 36, p. L23401, 2009.

[16] J. Heiskanen, "Tree cover and height estimation in the Fennoscandian tundra-taiga transition zone using multiangular MISR data," *Remote Sens. Environ.*, vol. 103, pp. 97–114, 2006.

[17] D. S. Kimes, K. J. Ranson, G. Sun, and J. B. Blair, "Predicting lidar measured forest vertical structure from multi-angle spectral data," *Remote Sens. Environ.*, vol. 100, pp. 503–511, 2006.

[18] J.-L. Widlowski, B. Pinty, N. Gobron, M. Verstraete, D. J. Diner, and B. Davis, "Canopy structure parameters derived from multi-angular remote sensing data for terrestrial carbon studies," *Climatic Change*, vol. 67, pp. 403–415, 2004.

[19] M. A. Schull, S. Ganguly, A. Samanta, D. Huang, N. V. Shabanov, J. P. Jenkins, J. C. Chiu, A. Marshak, J. B. Blair, R. B. Myneni, and Y. Knyazikhin, "Physical interpretation of the correlation between multi-angle spectral data and canopy height," *Geophys. Res. Lett.*, vol. 34, p. L18405, 2007, doi 10.1029/2007GL031143.

[20] Y. Zeng and M. E. Schaepman, "Quantitative forest canopy structure assessment using an inverted geometric-optical model and up-scaling," *Int. J. Remote Sens.*, vol. 30, no. 6, pp. 1385–1406, 2009.

[21] M. Chopping, G. Moisen, L. Su, A. Laliberte, A. Rango, J. V. Martonchik, and D. P. C. Peters, "Large area mapping of southwestern forest crown cover, canopy height, and biomass using MISR," *Remote Sens. Environ.*, vol. 112, pp. 2051–2063, 2008.

[22] M. Chopping, A. W. Nolin, G. G. Moisen, J. V. Martonchik, and M. Bull, "Forest canopy height from the Multiangle Imaging Spectro-Radiometer (MISR) assessed with high resolution discrete return lidar," *Remote Sens. Environ.*, vol. 113, pp. 2172–2185, 2009.

[23] M. Chopping, C. B. Schaaf, F. Zhao, Z. Wang, A. W. Nolin, G. G. Moisen, J. V. Martonchik, and M. Bull, "Forest structure and aboveground biomass in the southwestern United States from MODIS and MISR," *Remote Sens. Environ.*, vol. 115, pp. 2943–2953, 2011.

[24] Z. Wang, C. B. Schaaf, P. Lewis, Y. Knyazikhin, M. A. Schull, A. H. Strahler, T. Yao, R. B. Myneni, and M. Chopping, "Retrieval of canopy vertical structure using MODIS data," *Remote Sens. Environ.*, vol. 115, no. 6, pp. 1595–1601, 2011.

[25] V. C. E. Laurent, W. Verhoef, J. G. P. W. Clevers, and M. E. Schaepman, "Inversion of a coupled canopy-atmosphere model using multi-angular top-of-atmosphere radiance data: A forest case study," *Remote Sens. Environ.*, vol. 115, pp. 2603–2612, 2011.
[26] K. J. Ranson, C. S. T. Daughtry, L. L. Biehl, and L. L. , "Sun angle, view angle, and background effects on spectral response of simulated balsam fir canopies," *Photogramm. Eng. Remote Sens.*, vol. 52, pp. 649–658, 1986.
[27] F. Gemmell, "Testing the utility of multi-angle spectral data for reducing the effects of background spectral variations in forest reflectance model inversion," *Remote Sens. Environ.*, vol. 72, pp. 46–63, 2000.
[28] J. Pisek and J. M. Chen, "Mapping forest background reflectivity over North America with Multi-angle Imaging SpectroRadiometer (MISR) data," *Remote Sens. Environ.*, vol. 113, no. 11, pp. 2412–2423, 2009.
[29] U.S. Forest Service, Interior West FIA Geospatial Products— 2005, IW-FIA metadata document [Online]. Available: http://www.fs.fed.us/rm/ogden/map-products/intwest/map_pdfs/iw_models_2005_metadata.pdf, (latest access 01/11/09), 2005
[30] M. J. Chopping, S. Shimada, M. Bull, and J. Martonchik, "Canopy height, crown cover, and aboveground biomass maps for the southwestern United States from MISR, 2000 and 2009," in *Proc. 2010 IEEE Int. Geoscience and Remote Sensing Symp.*, Honolulu, Hawaii, Jul. 25–30, 2010, pp. 56–59.
[31] M. Chopping, "CANAPI: Canopy analysis with panchromatic imagery," *Remote Sens. Lett.*, vol. 2, no. 1, pp. 21–29, 2010.
[32] M. North and J. Chen, "Introduction to the special issue on Sierran mixed-conifer research," *Forest Sci.*, vol. 51, no. 3, pp. 185–186, 2005.
[33] W. H. McNab and P. E. Avers, Eds., "Ecological Subregions of the United States," U.S. Forest Service [Online]. Available: http://www.fs.fed.us/land/pubs/ecoregions/ch33.html#M261E, (last accessed on August 31, 2011), 1994
[34] D. J. Diner, G. P. Asner, R. Davies, Y. Knyazikhin, J.-P. Muller, A. W. Nolin, B. Pinty, C. B. Schaaf, and J. Stroeve, "New directions in Earth observing: Scientific applications of multiangle remote sensing," *B. Am. Meteorol. Soc.*, vol. 80, no. 11, pp. 2209–2229, 1999.
[35] D. J. Diner, W. A. Abdou, T. P. Ackerman, K. Crean, H. R. Gordon, R. A. Kahn, J. V. Martonchik, S. McMuldroch, S. R. Paradise, B. Pinty, M. M. Verstraete, M. Wang, and R. A. West, "MISR Level-2 Aerosol Retrieval Algorithm Theoretical Basis Document," Jet Propulsion Lab., California Institute of Technology, 2008.
[36] M. North, J. Chen, B. Oakley, B. Song, M. Rudnicki, and A. Gray, "Forest stand structure and pattern of old-growth western hemlock/Douglas-fir and mixed-conifer forests," *Forest Sci.*, vol. 50, no. 3, pp. 299–311, 2004.
[37] P. Maloney, T. Smith, C. Jensen, J. Innes, D. Rizzo, and M. North, "Initial tree mortality, and insect and pathogen response to fire and thinning restoration treatments in an old growth, mixed-conifer forest of the Sierra Nevada, California," *Can. J. Forest Res.*, vol. 38, pp. 3011–3020, 2008.
[38] J. B. Blair, M. A. Hofton, and D. L. Rabine, "Processing of NASA LVIS Elevation and Canopy (LGE, LCE and LGW) Data Products," ver. 1.01 [Online]. Available: http://lvis.gsfc.nasa.gov, 2006
[39] A. H. Strahler, D. L. B. Jupp, C. E. Woodcock, and X. Li, "The discrete-object scene model and its application in remote sensing," in *Proc. Int. Symp. Physical Measurements and Signature in Remote Sensing*, Beijing, China, 2005.
[40] X. Li and A. H. Strahler, "Geometric-optical modeling of a conifer forest canopy," *IEEE Trans. Geosci. Remote Sens.*, vol. 23, pp. 705–721, 1985.
[41] J. M. Chen, X. Li, T. Nilson, and A. Strahler, "Recent advances in geometrical optical modeling and its applications," *Remote Sens. Rev.*, vol. 18, pp. 227–262, 2000.
[42] J.-L. Roujean, M. Leroy, and P.-Y. Deschamps, "A bidirectional reflectance model of the Earth's surface for the correction of remote sensing data," *J. Geophys. Res.*, vol. 97, no. D18, pp. 20455–20468, 1992.
[43] W. Wanner, X. Li, and A. H. Strahler, "On the derivation of kernels for kernel-driven models of bidirectional reflectance," *J. Geophys. Res.*, vol. 100, pp. 21077–21090, 1995.
[44] J. K. Ross, *The Radiation Regime and Architecture of Plant Stands*. The Hague: Dr. W. Junk Publishers, 1981, p. 392.
[45] J. E. Luther and A. L. Carroll, "Development of an index of balsam fir vigor by foliar spectral reflectance," *Remote Sens. Environ.*, vol. 69, no. 3, pp. 241–252, 1999.
[46] C. L. Walthall, J. M. Norman, J. M. Welles, G. Campbell, and B. L. Blad, "Simple equation to approximate the bidirectional reflectance from vegetative canopies and bare surfaces," *Appl. Optics*, vol. 24, pp. 383–387, 1985.
[47] T. Nilson and A. Kuusk, "A reflectance model for the homogenous plant canopy and its inversion," *Remote Sens. Environ.*, vol. 27, pp. 157–167, 1989.
[48] A. H. Strahler, W. Wanner, C. Schaaf, X. Li, B. Hu, J.-P. Muller, P. Lewis, and M. Barnsley, MODIS BRDF/albedo Product: Algorithm Theoretical Basis Documentation ver. 4.0, NASA/EOS ATBD, p. 94, 1996.
[49] W. Yang, W. Ni-Meister, and S. Lee, "Assessment of the impacts of surface topography, off-nadir pointing and vegetation structure on vegetation lidar waveforms using an extended geometric optical and radiative transfer model," *Remote Sens. Environ.*, vol. 115, pp. 2810–2822, 2011.
[50] J. Nocedal and S. J. Wright, *Numerical Optimization*. New York: Springer-Verlag, 1999, p. 636, 0-387-98793-2.

Mark Chopping received the M.Phil. degree in remote sensing and geographical information systems from the University of Cambridge, U.K., in 1995 and the Ph.D. in remote sensing from the University of Nottingham, U.K., in 1998.

From 1999 to 2002, he served as a Physical Scientist with the Agricultural Research Service, United States Department of Agriculture, and from 2000 as principal investigator in the ESA CHRIS/Proba mission (Data Exploitation Phase). In 2002, he joined the Department of Earth and Environmental Studies at Montclair State University, Montclair, NJ, where he is currently a Professor. He served on the NASA Land Cover Land Use Change Science Team from 2004 to 2008 and is currently a member of the NASA Terrestrial Ecology Science Team, the NASA MISR Science Team, and the NASA MODIS Science Team. He also serves as principal investigator in the multi-agency North American Carbon Program. Dr. Chopping's research interests include the interpretation of MISR and MODIS data with canopy reflectance and BRDF models to enhance mapping of vegetation canopies, with foci in arid and semi-arid regions, desert grasslands, western forests, and Arctic tundra.

Malcolm North received the Ph.D. in forest ecology from the University of Washington, Seattle, in 1993 and the M.S. degree in forest science from Yale University, New Haven, CT, in 1988.

He is a Research Scientist with the USDA Forest Service, Pacific Southwest Research Station, Davis, CA, and an Adjunct Professor of forest ecology with the Department of Plant Sciences, University of California, Davis. He is the Principal Investigator for the Teakettle Ecosystem Experiment in the Sierra Nevada and author of several papers on the forest ecology of mixed-conifer forests. His interests are in the effects of disturbance on forest ecosystem processes and wildlife habitat and he is actively involved in developing new methods for managing fire-dependent forests in the Sierra Nevada.

Dr. North is a member of the Ecological Society of America and Fire Ecologists Association. He also teaches and mentors graduate students in UC Davis's Graduate Group in Ecology. He has received awards for science productivity and outreach from the U.S. Forest Service.

Jiquan Chen received the Ph.D. in ecosystem analysis from the University of Washington, Seattle, in 1991 and the M.S. degree in forest ecology, from the Chinese Academy of Sciences, Beijing and Shenyang, China in 1986.

He is currently a Distinguished University Professor in ecology at the University of Toledo, Canada. He is broadly interested in ecosystem science and landscape ecology. He has conducted substantial research on forest edges, three dimensional canopy structure, ecosystem carbon and water fluxes, energy balance, riparian zone management, fire ecology, and hierarchical landscape analysis. Dr. Chen's current research is on coupled influences of climate change and human activities on ecosystem functions at various temporal and spatial scales.

Crystal B. Schaaf (M'92) received the S.B. and S.M. degrees in meteorology from the Massachusetts Institute of Technology, Cambridge, in 1982, the M.L.A. degree in archaeology from Harvard University, Cambridge, in 1988, and the Ph.D. degree in geography in 1994 from Boston University, Boston, MA.

She is currently a Professor in the Environmental, Earth and Ocean Sciences Department at the University of Massachusetts, Boston. She works on the development and use of operational products from NASA's MODerate Resolution Imaging Spectrometer (MODIS) to monitor the Earth's environments from the Terra and Aqua polar-orbiting space platforms. She is a science team member for both MODIS and the VIIRS (Visible Infrared Imaging Radiometer Suite) sensor on board NPP the first of the next generation of national meteorological satellites). Her early research focused the use of remote sensing in automated cloud analyses and the detection of initiating convective clouds. Dr. Schaaf's current interests include modeling reflectance anisotropy and albedo and using remote sensing data to reconstruct and monitor the reflectance characteristics of various land surfaces, including vegetation phenology and land surface change. More recently she has also been involved in the development and use of ground-based lidar systems to characterize biomass and vegetation structure.

J. Bryan Blair received the B.Sc. degree in mathematics from Towson State University, Towson, MD, in 1987, and the M.S. degree in computer engineering from Loyola College, Baltimore, MD, in 1989.

Since 1989, he has been with the Laser Remote Sensing Laboratory, NASA Goddard Space Flight Center, Greenbelt, MD, where he has worked on numerous airborne and spaceborne lidars. He was the Flight Software Lead for the Mars Orbital Laser Altimeter (MOLA) that successfully mapped the surface topography of Mars. For the Shuttle Laser Altimeters (SLA-01, and -02) he served as the Instrument Scientist and altimetry lead. He was a member of the Lunar Orbital Laser Altimeter (LOLA) instrument design team and served as the Instrument Scientist for the DESDynI Lidar. He is currently Principal Investigator for the Land, Vegetation, and Ice Sensor (LVIS), for LVIS mapping projects in Greenland and Antarctica for the Operation IceBridge Project. His interests include development of new laser altimeter techniques to allow large-area mapping from high-altitude aircraft and, eventually, complete Earth surface mapping from space, as well as advanced algorithms and data analysis techniques for waveform lidar for vegetation measurements, surface change detection, and the production of highly accurate digital elevation models.

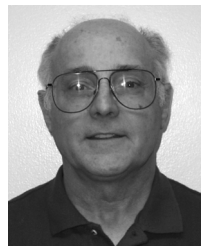

John V. Martonchik received the B.S. degree in physics from Case Institute of Technology in 1964 and the Ph.D. degree in astronomy from the University of Texas in 1975.

He has been with the Jet Propulsion Laboratory, California Institute of Technology, since 1972 and is currently a Co-Investigator and the algorithm scientist for aerosol and surface retrievals on MISR. His experiences include telescopic and spacecraft-based observations of planetary atmospheres, laboratory and theoretical studies of the optical properties of gaseous, liquid and solid materials, and development and implementation of one- and three-dimensional radiative transfer and line-by-line spectroscopy algorithms for studies of planetary atmospheres and Earth tropospheric remote sensing.

Michael A. Bull received the B.S. degree (with honors) in computer science from the University of Maryland, College Park, in 1992 and the M.S. degree in computer science from the University of California, Los Angeles, in 1994.

He is currently providing software development support for MISR in the areas of geometric calibration and registration, and aerosol science algorithms. He has been with the Jet Propulsion Laboratory, Pasadena, CA, since 1996, working as a member of the software development team for the Multi-angle Imaging SpectroRadiometer (MISR) project.